AD-A145 893 STRESS INTENSITY FACTORS FOR A CIRCULAR RING WITH UNIFORM ARRAY OF RADIAL..(U) ARMY ARMAMENT RESEARCH AND DEVELOPMENT CENTER WATERVLIET NY L.. S L PU JUN 84 1/1

UNCLASSIFIED ARLCB-TR-84021 SBI-AD-E440 252 F/G 20/11 NL

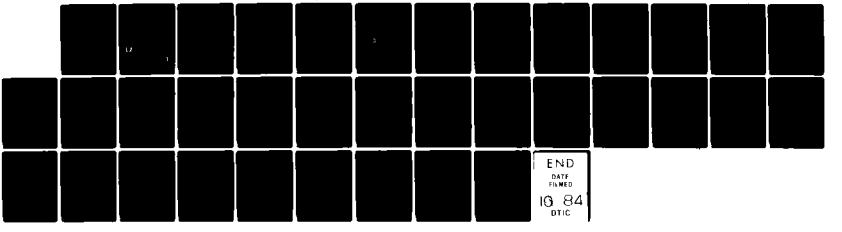

END
DATE FILMED
10 84
DTIC

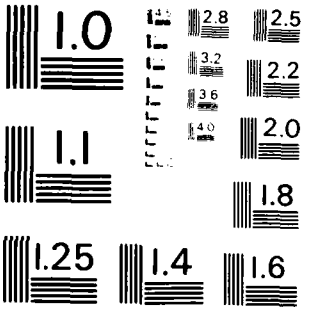

(12)

TECHNICAL REPORT ARLCB-TR-84021

STRESS INTENSITY FACTORS FOR A CIRCULAR RING WITH UNIFORM ARRAY OF RADIAL CRACKS OF UNEQUAL DEPTH

S. L. PU

JUNE 1984

US ARMY ARMAMENT RESEARCH AND DEVELOPMENT CENTER
LARGE CALIBER WEAPON SYSTEMS LABORATORY
BENET WEAPONS LABORATORY
WATERVLIET N.Y. 12189

DISCLAIMER

The findings in this report are not to be construed as an official Department of the Army position unless so designated by other authorized documents.

The use of trade name(s) and/or manufacture(s) does not constitute an official indorsement or approval.

DISPOSITION

Destroy this report when it is no longer needed. Do not return it to the originator.

9 August 1984

ERRATA SHEET
(Change Notice)

CI TO: TECHNICAL REPORT ARLCB-TR-84021

STRESS INTENSITY FACTORS FOR A CIRCULAR RING WITH UNIFORM ARRAY OF RADIAL CRACKS OF UNEQUAL DEPTH

by

S. L. Pu

Please insert Page 25 in the above Technical Report. *This page was inadvertently omitted* from the original publication.

US ARMY ARMAMENT RESEARCH AND DEVELOPMENT CENTER

LARGE CALIBER WEAPON SYSTEMS LABORATORY

BENET WEAPONS LABORATORY

WATERVLIET, N. Y. 12189

SECURITY CLASSIFICATION OF THIS PAGE *(When Data Entered)*

REPORT DOCUMENTATION PAGE		READ INSTRUCTIONS BEFORE COMPLETING FORM
1. REPORT NUMBER ARLCB-TR-84021	2. GOVT ACCESSION NO. AD-A145893	3. RECIPIENT'S CATALOG NUMBER
4. TITLE *(and Subtitle)* STRESS INTENSITY FACTORS FOR A CIRCULAR RING WITH UNIFORM ARRAY OF RADIAL CRACKS OF UNEQUAL DEPTH		5. TYPE OF REPORT & PERIOD COVERED Final 6. PERFORMING ORG. REPORT NUMBER
7. AUTHOR(s) S. L. Pu		8. CONTRACT OR GRANT NUMBER(s)
9. PERFORMING ORGANIZATION NAME AND ADDRESS US Army Armament Research & Development Center Benet Weapons Laboratory, DRSMC-LCB-TL Watervliet, NY 12189		10. PROGRAM ELEMENT, PROJECT, TASK AREA & WORK UNIT NUMBERS AMCMS NO.6111.02.H600.011 PRON NO. 1A325B541A1A
11. CONTROLLING OFFICE NAME AND ADDRESS US Army Armament Research & Development Center Large Caliber Weapon Systems Laboratory Dover, NJ 07801		12. REPORT DATE June 1984 13. NUMBER OF PAGES 27
14. MONITORING AGENCY NAME & ADDRESS*(if different from Controlling Office)*		15. SECURITY CLASS. *(of this report)* UNCLASSIFIED 15a. DECLASSIFICATION/DOWNGRADING SCHEDULE

16. DISTRIBUTION STATEMENT *(of this Report)*

Approved for Public Release; Distribution Unlimited

17. DISTRIBUTION STATEMENT *(of the abstract entered in Block 20, if different from Report)*

18. SUPPLEMENTARY NOTES

Presented at Second Conference on Applied Mathematics & Computing, RPI, Troy, NY, 22-24 May 1984. To be published in the Proceedings of same conference.

19. KEY WORDS *(Continue on reverse side if necessary and identify by block number)*

Stress Intensity Factors
Multiple Cracks
Cracks of Unequal Lengths
Fracture Mechanics
Thick-Wall Cylinders

20. ABSTRACT *(Continue on reverse side if necessary and identify by block number)*

The plane problem of a uniform array of unequal depth radial cracks originating at the internal boundary of a pressurized circular ring is considered. The 12-node quadrilateral isoparametric elements with collapsed singular elements around crack tips are used to compute stress intensity factors at crack tips.

(CONT'D ON REVERSE)

DD FORM 1 JAN 73 1473 EDITION OF 1 NOV 65 IS OBSOLETE UNCLASSIFIED

SECURITY CLASSIFICATION OF THIS PAGE *(When Data Entered)*

20. ABSTRACT (CONT'D)

In a previous study of equal depth radial cracks, the weakest configuration is a ring with two diametrically opposed cracks. The current study shows that if for any reason one of the two cracks should grow a little faster than the other, the stress intensity factor at the tip of the longer crack increases at a much faster rate to enhance the faster growth of the longer crack.

Numerical results are also obtained for cases of three and four radial cracks. It shows the same trend that once one or two cracks grow a little more than the rest, the stress intensity factors at these deeper cracks will be increased progressively higher to keep the faster pace of growth. This explains why the failure caused by a single major crack has been observed most frequently.

A simple linear relation is assumed in this report between the stress intensity ratio and the crack depth ratio. This approximation enables us to estimate stress intensity factors at unequal depth cracks by a method of total differentials. The estimations thus obtained are close to stress intensity factors computed from the finite element.

TABLE OF CONTENTS

TABLES

LIST OF ILLUSTRATIONS

INTRODUCTION

A series of efforts has been made to estimate stress intensity factors of radial cracks in a cylindrical pressure vessel. In order to facilitate the finite element computations of such a cracked cylinder, a collapsed 12-node triangular element with nodes shifted to 1/9 and 4/9 locations was developed in Reference 1. The use of these elements around a crack tip has helped in computing stress intensity factors for an array of uniformly distributed radial cracks of equal depth emanating from the inner surface of a thick-walled tube. Our finite element results, reported in Reference 2, are in good agreement with results obtained by other methods (refs 3-5). To reduce stress intensity factors at these cracks so the fatigue life of the pressure vessel may be prolonged, it becomes a common practice to use the autofrettage process. This process produces a residual stress in a cylinder following plastic deformation and elastic unloading. The residual stress is compressive near the bore and is tensile near the outer surface. While it is useful to retard the growth of cracks near the bore where the residual compressive stress reduces the maximum tensile stress level due to a bore pressure, it may cause problems at cracks near the outer surface where the final stress becomes the sum of residual tensile stress and the tensile stress due to a pressure loading applied at the bore. There must be an optimal degree of autofrettage when failures from both inner and outer cracks are equally likely. The computations of stress intensity factors at inner and outer cracks are more involved if a cylinder undergoes a partial autofrettage.

References are listed at the end of this report.

One of the difficulties is the discrepancy among predictions on residual stress distribution by different investigators based on different assumptions. References 6 through 13 represent a partial list of works on this subject. Another difficulty is the lack of an existing general purpose finite element computer code which has the feature of treating an arbitrary initial stress distribution. To develop a method of computing stress intensity factors in this situation, the closed form expressions for residual stresses for an incompressible, elastic-ideally plastic material (ref 7) are chosen. In addition, an equivalent thermal load was found in Reference 14 which can be prescribed at the nodes of the existing computer codes NASTRAN and APES (ref 15) to avoid the need of modification of computer codes in order to handle initial stresses. A summary of these methods and some results in stress intensity computations for cracks in a partially autofrettaged cylinder is given in Reference 16. Other efforts on this subject are given in References 17 and 18. Further extension of the method developed for radial cracks in cylindrical pressure vessels of elastic-perfectly plastic materials to similar cracks of strain-hardening materials is published in Reference 19.

Thus far the stress intensity factors have been obtained for uniformly distributed radial cracks of equal depth. The weakest configuration was found to be two diametrically opposite cracks in non-autofrettaged cylinders. For autofrettaged cylinders, the weakest configuration is dependent on the degree of autofrettage and the ratio of bore pressure to yield strength. It remains true in general that two diametrically opposite cracks make a cylinder the least resistant to fracture. However, from the actual observations of fracture of thick-walled tubes, it is a single major crack which has caused

the failure most frequently. The objective of this study is to compute the change in stress intensity factors at different crack tips when they grow from an equal depth configuration to an unequal depth configuration. Based on some finite element computations of stress intensity factors, a numerical method is needed to estimate stress intensity factors at each crack tip of a cracked tube when radial cracks are unequal depths. Results in this report are limited to non-autofrettaged, pressurized tubes. However, it is not difficult to extend the method to partially autofrettaged tubes. Results will appear in a separate report.

FINITE ELEMENT RESULTS OF STRESS INTENSITY

The 12-node quadrilateral isoparametric elements were used in this study. The shape functions and the mathematical formulation of the element stiffness matrix are given in Reference 1. The crack tip elements are formed by collapsing the quadrilateral elements into triangular elements around the crack tip. On each side of a triangle emitting from the crack tip, the locations of intermediate nodes are shifted from their usual 1/3 and 2/3 of the length of the side to 1/9 and 4/9 of the length measured from the tip. This simple technique gives the required singularity of the strain field at the crack tip (ref 1). The stress intensity factors can be computed quite accurately from certain nodal displacements (ref 1). A general purpose computer program having isoparametric elements such as NASTRAN may be used for our study. However, the computer code APES is chosen due to many convenient features of the program.

Using similar notations as in Reference 2, n denotes the number of radial cracks, W is the wall ratio, R_2/R_1, where R_1 and R_2 are inner and outer radii of the ring, respectively. The thickness of the wall, $t = R_2 - R_1$, is used to normalize the crack depth a. The dimensionless crack depth a/t is denoted by c. A subscript i, i = 1,2,...n, is used to name a crack. Let the Cartesian coordinates be chosen such that the origin is at the center of the ring and a radial crack lies on the positive x-axis. This crack is assigned the number one. The crack number increases counterclockwise from the x-axis. In this study our finite element computations are limited to W = 2 and n = 2, 3 and 4 as shown in Figure 1. Starting from equal depth crack configuration, we proceed to unequal depth configurations by a systematic increment of crack depth of one, two, or three cracks. For a given n, let c and K_e be the crack depth and stress intensity factor, respectively, when all cracks are of the same depth. These quantities are used to normalize the crack depth c_i and the mode I stress intensity factor K_I for the i-th crack when cracks become unequal depths. New notations p and N are introduced for these dimensionless quantities

$$p_i = c_I/c \quad , \quad N_I = K_I/K_e \qquad i = 1,2,...n \tag{1}$$

It is true that some cracks are under mixed mode I and mode II conditions when unequal-depth-crack configurations are considered. However, in this study the effect of the shear mode is assumed to be negligible and only the dominant mode I stress intensity factors are considered.

The idealizations used in this study for a ring with two, three, and four cracks are shown in Figures 2, 3, and 4, respectively. Only the upper half of a ring is shown due to symmetry consideration in finite element computations.

Equilateral triangles are used around a crack tip and these collapsed singular elements are surrounded by a layer of quadrilateral elements, detail A of Figure 2 and detail B of Figure 3. The finite element results of K_e using the refined meshes are shown in Figure 5 and are very close to results previously obtained in Reference 2 using slightly different meshes around a crack tip.

For two diametrically opposed radial cracks, stress intensity factors are computed for various lengths of c_1 with a fixed value of $c_2 = c = 0.2$. In a graph of N_i, $i = 1$ and 2, versus ρ_1, Figure 6, finite element results are shown as dots. It can be seen that the dots may be joined approximately by straight lines. Similar results are also obtained and shown in the same graph for $c_2 = c = 0.3$.

For three radial cracks, the crack 2 and crack 3 remain the mirror image of each other so that the problem is symmetric with respect to the x-axis. Two subcases are considered. In the first case, the crack depths of both crack 2 and crack 3 are fixed at $c_2 = c_3 = c = 0.2$ or 0.3. Stress intensity factors at crack tips of crack 1 and crack 2 are computed for various values of ρ_1. Finite element results are shown as dots for $c = 0.2$ and as crosses for $c = 0.3$ in Figure 7. In the second case, the first crack has a fixed crack depth and the other two cracks grow simultaneously at the same rate. Finite element results for the latter case are used only for the purpose of checking our numerical approximations.

In the case of four radial cracks, crack 4 is kept as the mirror image of crack 2. This symmetry reduces the problem to the upper half of the ring with three cracks. There are three subcases which have been studied. The first case is that only crack 1 grows. In the second subcase, crack 1 and crack 3

are growing simultaneously at the same rate and crack 2 has a fixed crack depth. The third case is just opposite to the first case. The crack 1 is fixed in length with crack 2 and crack 3 growing at the same rate. Using the idealization shown in Figure 4, finite element results of stress intensity factors are obtained at each crack tip for various increments in crack depth of the growing crack or cracks. The results for the first subcase are shown as dots and crosses in Figure 8. The numerical results for the other two subcases are not given since they are used only for checking the numerical approximations by total differentials.

APPROXIMATION BY TOTAL DIFFERENTIALS

We assume that the differential change in stress intensity factor at crack i due to the differential change in length of crack j may be given by

$$dN_i = \frac{\partial N_i}{\partial \rho_j} d\rho_j \tag{2}$$

The change in stress intensity factor due to a small change from ρ_j to $\rho_j + \Delta\rho_j$ can be expressed by

$$\Delta N_i = \int_{\rho_j}^{\rho_j+\Delta\rho_j} \frac{\partial N_i}{\partial \rho_j} d\rho_j \tag{3}$$

If the increment $\Delta\rho_j$ is divided into m_j intervals

$$\Delta\rho_j = \Delta_1\rho_j + \Delta_2\rho_j + \ldots + \Delta m_j\rho_j \tag{4}$$

and if in any interval ℓ there exists a quantity $(\partial N_i/\partial\rho_j)_\ell$ such that

$$\left(\frac{\partial N_i}{\partial \rho_j}\right)_\ell \Delta_\ell\rho_j = \int_{\rho_j+\Delta_{\ell-1}\rho_j}^{\rho_j+\Delta_\ell\rho_j} \frac{\partial N_i}{\partial \rho_j} d\rho_j \tag{5}$$

The integral at the right hand side of Eq. (3) may be replaced by a summation

$$\Delta N_i = \sum_{\ell=1}^{m_j} \left(\frac{\partial N_i}{\partial \rho_j}\right)_\ell \Delta_\ell \rho_j \tag{6}$$

Furthermore, if the change in stress intensity factor at crack tip i due to simultaneous changes in length of two or more cracks may be approximated as the sum of changes due to each crack length change, then the total change of stress intensity factor at crack i due to length changes of all cracks may be approximately expressed by

$$\Delta N_i = \sum_{j=1}^{n} \sum_{\ell=1}^{m_j} \left(\frac{\partial N_i}{\partial \rho_j}\right)_\ell \Delta_\ell \rho_j \tag{7}$$

The partial derivative $(\partial N_i/\partial \rho_j)_\ell$ may be calculated from the slope of the tangent to the curve of N_i versus ρ_j which is obtained by curve fitting of discreted points in the ρ-N plane from the finite element computations. The change in N_i must be restricted to that due to the change in ρ_j only. Figures 6 through 8 are used for this purpose with finite element values of N_i obtained for various values of ρ_l with the crack depth of all other cracks fixed. A study of data points (ρ,N) in Figures 6 through 8 shows that a straight line of the form

$$N-1 = m(\rho-1) \tag{8}$$

fits these points in a close approximation. The slope m of a least square regression is given by

$$m = \sum_i (N_i-1)(\rho_i-1) / \sum_i (\rho_i-1)^2 \tag{9}$$

This slope may be used as the average value of the partial derivatives $\partial N_i/\partial \rho_i$ in a proper range of ρ_l for a given set of values n and c. For n = 2, 3, and 4, the slopes m of linear regressions are computed and shown in Figures 6

through 8 for c = 0.2 or c = 0.3 in a range $1 < \rho_1 < 1.8$.

For a given equal depth crack configuration we have

$$\frac{\partial N_i}{\partial \rho_i} = \frac{\partial N_j}{\partial \rho_j} \quad , \quad \frac{\partial N_i}{\partial \rho_j} = \frac{\partial N_j}{\partial \rho_i} \qquad (i,j = 1,2,\ldots n) \tag{10}$$

Stress intensity factor at any crack tip of unequal radial cracks may be estimated by using Eqs. (7) and (10). The approximate method is applied to subcase 2 of n = 3 and subcases 2 and 3 of n = 4. The results are compared to finite element results and the difference is in general less than four percent. Two examples of the comparison are given in Table I. In both examples the depth of crack 1 was held constant and the depth of all other cracks increased an amount of forty percent of the depth of crack 1.

TABLE I. COMPARISON OF $K_I/p\sqrt{R_1}$, FINITE ELEMENT RESULTS VERSUS APPROXIMATIONS

No. of Crack	Crack Depth		i = 1		i = 2		i = 3	
n	c_1	Other c	F.E.	Approx.	F.E.	Approx.	F.E.	Approx.
3	0.2	0.28	2.26	2.29	2.69	2.70	2.69	2.70
4	0.3	0.42	2.52	2.52	3.60	3.50	3.02	2.97

In the previous example of four-crack case, the stress intensity factor of 3.6 at crack 2 or 4 is well above 3.3, the would be value if crack 1 has not arrested but grew at the same rate. The stress intensity factor at crack 2 due to the presence of crack 1 and 3 is considerably lower than 4.2, the stress intensity factor for two-crack case with c = 0.42. The faster increase in stress intensity factor at crack 2 and crack 4, however, tends to change the four-crack configuration to a crack configuration dominated by two cracks.

The approximate method may be used to obtain results for crack configurations which are more difficult to compute by the finite element method. For instance, a ring with three radial cracks of different depths, say $c_1 = 0.2$, $c_2 = 0.26$, and $c_3 = 0.3$, the entire ring with three crack tips has to be considered by the finite element method. The method of total differentials can easily yield the following estimates: $N_1 = 1.025$, $N_2 = 1.166$, and $N_3 = 1.26$. Taking $K_e/p\sqrt{R_1} = 2.23$ from Figure 5 for $n = 3$, $c = 0.2$, we have $K_1/p\sqrt{R_1} = 2.28$, $K_2/p\sqrt{R_1} = 2.60$, and $K_3/p\sqrt{R_1} = 2.81$.

For a given value of n, if we obtain $\partial N/\partial p$ for many values of c, then a plot of $\partial N/\partial p$ versus c may be obtained. Such a plot for $n = 3$ is shown in Figure 9. It shows that $\partial N_1/\partial p_1$ is nearly a linear function of c. Let $\partial N_2/\partial p_1$ be a quadratic function of c of the form

$$\partial N_2/\partial p_1 = m' c^2 \tag{11}$$

The curve which best fits data in the least square sense is given by

$$m' = \sum_i c_1^2 (\partial N_2/\partial p_1)_i / \sum_i c_1^4 \tag{12}$$

For the curve in Figure 9, m' is approximately 0.577. The equation of the linear regression in Figure 9 is

$$\partial N_1/\partial p_1 = 1.077\ c + 0.296 \tag{13}$$

A plot such as Figure 9 or equations similar to Eqs. (11) and (13) may be used to obtain approximate values of $\partial N_1/\partial p_1$ at a specific value of c for which no finite element results are available. Using $\partial N_1/\partial p_1 = 0.4037$ and $\partial N_2/\partial p_1 = 5.77 \times 10^{-3}$ for $n = 3$, $c = 0.1$ in Eqs. (7) and (10) and taking $K_e/p\sqrt{R_1} = 1.56$ from Figure 5, our estimations are $K_1/p\sqrt{R_1} = 1.563$, $K_2/p\sqrt{R_1} = 1.438$ and $K_3/p\sqrt{R_1} = 1.873$ for the three-crack case of $c_1 = 0.1$, $c_2 = 0.08$, and $c_3 =$

0.15. In our computation a negative value of -0.2 was used for $\Delta\rho_2$ in Eq. (7) to indicate the decrease in length of crack 2. The final estimation of stress intensity factors depends slightly on the judicious choice of c. In general, we take the smallest value of all crack lengths as c. In the previous example, if c = 0.08 is used, then c_3 would have a length increment of more than 80 percent. The estimations would have been $K_1/p\sqrt{R_1} = 1.538$, $K_2/p\sqrt{R_1} = 1.406$, and $K_3/p\sqrt{R_1} = 1.869$. The deviations in this example are relatively small. In some other cases the deviations become quite large when a length change is excessive. The choice of c for shallow cracks is more important and will be discussed in the following section.

APPROXIMATIONS FOR SHALLOW CRACKS

The finite element method has some difficulty in calculating stress intensity factors for very shallow cracks due to the small size of crack tip elements required to solve such problems. For c = 0.05, finite element results are available in Reference 16 for various n. For shallow cracks with $c < 0.05$, no finite element results are available since the accuracy of such computations is questionable. Some results for $c < 0.05$ were obtained by other methods. The most accurate results were reported in Reference 20 by MMC, the modified mapping collocation method. However, the approximate methods for shallow cracks discussed in Reference 21 are easy to use and yield reasonably accurate results. The crosses in the range $0 < c < 0.05$ in Figure 5 are obtained from the approximate formula (ref 22) for a single crack

$$K = \{1.12\ \sigma_\theta(r=R_1) - 0.68[\sigma_\theta(r=R_1) - \sigma_\theta(r=r_c)]\}\sqrt{\pi c} \qquad (14)$$

where $\sigma_\theta(r=R_1)$ and $\sigma_\theta(r=r_c)$ are hoop stresses of an uncracked cylinder at $r = R_1$ and $r = r_c$, respectively. r_c denotes the radius of the crack tip. Using them and finite element results for $c = 0.05$ as a guide, the curves in Figure 5 are extended in broken lines to the region $c < 0.1$. The extended curves agree well with available MMC results.

Using the approximate method described in the preceding section and values from Figures 5 and 9, stress intensity factors can be easily estimated for equally spaced shallow cracks. The judicious choice of c in shallow crack cases is very important. For small n and small c the crack interaction is weak. It is recommended to choose $c = c_1$ for the computation of K_1. For instance, $n = 3$, $c_1 = 0.01$, $c_2 = 0.02$, and $c_3 = 0.03$, we obtain $K_1/p\sqrt{R_1} = 0.52$ by assuming the final crack configuration is reached from $c_1 = c_2 = c_3 = c = 0.01$. In the computation of K_2, we assume the final crack configuration is reached from $c_1 = c_2 = c_3 = c = 0.02$. The result is $K_2/p\sqrt{R_1} = 0.73$. For K_3, initial crack length $c = 0.03$ is assumed, depths of crack 1 and crack 2 are decreased from 0.03 to $c_1 = 0.01$ and $c_2 = 0.02$, the computed result is $K_3/p\sqrt{R_1} = 0.90$. The corresponding results by using Eq. (14) are $K_1/p\sqrt{R_1} = 0.53$, $K_2/p\sqrt{R_1} = 0.74$, and $K_3/p\sqrt{R_1} = 0.90$. Another easier alternative method for shallow cracks is the use of stress intensity factors for equal-depth cracks. For $n = 3$, when all crack depths are $c = 0.01$, the stress intensity factor at a crack tip is $K/p\sqrt{R_1} = 0.52$. Similarly $K/p\sqrt{R_1} = 0.73$ for $c = 0.02$ and $K/p\sqrt{R_1} = 0.90$ for $c = 0.03$. Using these values to the crack of the right crack depth in the unequal-depth crack configuration, all three approximate methods for shallow cracks are useful up to $c = 0.1$. As a last example, $n = 3$, $c_1 = 0.05$, $c_2 = 0.07$, and $c_3 = 0.09$, the first method gives $K_1/p\sqrt{R_1} =$

1.122, $K_2/p\sqrt{R_1} = 1.31$, and $K_3/p\sqrt{R_1} = 1.495$. Equation (14) gives $K_1/p\sqrt{R_1} = 1.15$, $K_2/p\sqrt{R_1} = 1.347$, and $K_3/p\sqrt{R_1} = 1.512$. The use of equal crack depth results gives $K_1/p\sqrt{R_1} = 1.12$, $K_2/p\sqrt{R_1} = 1.31$, and $K_3/p\sqrt{R_1} = 1.50$.

CONCLUSIONS

The 12-node quadrilateral isoparametric elements with collapsed singular elements around a crack tip can be used to efficiently compute stress intensity factors at tips of multiple radial cracks of unequal depths in a thick-walled cylinder. Based on finite element results of some selected crack configurations, the method of total differentials can estimate stress intensity factors accurately. The approximate method requires only a small number of finite element computations to obtain graphs such as Figure 7 and Figure 9 for a given n, then the method can estimate stress intensity factors for an arbitrary set of unequal cracks without the need of finite element computation for that particular crack configuration. The advantage of the approximate method is not only time saving, but also is able to give an estimate when the problem is not easily computed by the finite element method.

For shallow cracks, the stress intensity factor at a crack tip may be estimated from equal-depth crack configuration of that particular depth. This is due to the fact that the change in stress intensity factor at a shallow crack due to changes in crack depths of other shallow cracks is very small. Alternatively, each crack may be considered as a single crack since the interaction among shallow cracks is very weak. Hence the stress intensity factor at a crack tip is approximately proportional to the square root of the

crack depth. A deeper crack will have a higher stress intensity factor which in turn will cause further growth of the deeper crack. This process will change a large number of shallow cracks into a crack configuration consisting of several dominant cracks. Further, if one or two cracks are growing more than the rest, the increase in stress intensity factor at these deeper cracks is greater than the increase of others. This will reduce the number of dominant cracks and a single crack will eventually dominate. However, failure may occur before reaching the final stage of single crack domination.

Although no autofrettage residual stress has been considered in this study, the approximate method aided by the method summarized in Reference 23 may be used for partially autofrettaged, pressurized, multiply-cracked cylinders when crack depths are unequal.

REFERENCES

1. Pu, S. L., Hussain, M. A., and Lorensen, W. E., "The Collapsed Cubic Isoparametric Element as a Singluar Element For Crack Problems," Int. Journal for Numerical Methods in Engineering, Vol. 12, 1978, pp. 1727-1742.
2. Pu, S. L. and Hussain, M. A., "Stress Intensity Factors For a Circular Ring With Uniform Array of Radial Cracks Using Cubic Isoparametric Singular Elements," ASTM STP-677, 1979, pp. 685-699.
3. Bowie, O. L. and Freese, C. E., "Elastic Analysis For a Radial Crack in a Circular Ring," Engineering Fracture Mechanics, Vol. 4, 1972, pp. 315-321.
4. Grandt, A. F., "Two Dimensional Stress Intensity Factor Solutions For Radially Cracked Rings," Technical Report AFML-TR-75-121, Air Force Materials Laboratory, 1975.
5. Tracy, P. G., "Elastic Analysis of Radial Cracks Emanating From the Outer and Inner Surfaces of a Circular Ring," Engineering Fracture Mechanics, Vol. 11, 1979, pp. 291-300.
6. Davidson, T. E., Barton, C. S., Reiner, A. N., and Kendall, D. P., "Overstrain of High-Strength Open-End Cylinders of Intermediate Diameter Ratio," Proceedings of the First International Congress on Experimental Mechanics, Pergamon Press, Oxford, 1963, pp. 335-352.
7. Hill, R., The Mathematical Theory of Plasticity, Oxford at the Clarendon Press, 1950.

8. Hodge, P. G., and White, G. N., "A Quantitative Comparison of Flow and Deformation Theories of Plasticity," ASME Journal of Applied Mechanics, Vol. 72, 1950, pp. 180-184.

9. Weigle, R. E., "Elastic-Plastic Analysis of a Cylindrical Tube," Technical Report WVT-6007, Watervliet Arsenal, Watervliet, NY, 1960.

10. Chen, P. C. T., "Numerical Prediction of Residual Stresses in an Autofrettaged Tube of Compressible Material," Proceedings of the 1981 Army Numerical Analysis and Computer Conference, pp. 351-362.

11. Davidson, T. E. and Kendall, D. P., "The Design of Pressure Vessels for Very High Pressure Operation," Mechanical Behavior of Materials Under Pressure, H. L. P. Pugh, ed., Elsevier Co., 1970.

12. Chu, S. C., "A More Rational Approach to the Problem of an Elasto-Plastic Thick-Walled Cylinder," Journal of the Franklin Institute, Vol. 294, 1972, pp. 57-65.

13. Chen, P. C. T., "The Finite Element Analysis of Elastic-Plastic Thick-Walled Tubes," Proceedings of Army Symposium on Solid Mechanics, The Role of Mechanics in Design-Ballistic Problems, 1972, pp. 243-253.

14. Hussain, M. A., Pu, S. L., Vasilakis, J. D., and O'Hara, P., "Simulation of Partial Autofrettage by Thermal Loads," ASME Journal of Pressure Vessel Technology, Vol. 102, 1980, pp. 314-318.

15. Gifford, L. N., Jr., "APES - Second Generation Two-Dimensional Fracture Mechanics and Stress Analysis by Finite Elements," DTNSRDC Report 4799, 1975.

16. Pu, S. L. and Hussain, M. A., "Stress Intensity Factors For Radial Cracks in a Partially Autofrettaged Thick-Wall Cylinder," Proceedings of 14th National Symposium on Fracture Mechanics, 1981.

17. Kapp, J. A. and Eisenstadt, R., "Crack Growth in Externally Flawed, Autofrettaged Thick-Walled Cylinders and Rings," Fracture Mechanics, ASTM STP 677, 1979, pp. 746-756.

18. Parker, A. P., "Stress Intensity and Fatigue Crack Growth in Multiply-Cracked, Pressurized, Partially Autofrettaged Thick Cylinders," Fatigue of Engineering Materials and Structures, Vol. 4, No. 2, 1982.

19. Pu, S. L. and Chen, P. C. T., "Stress Intensity Factors For Radial Cracks in a Pre-Stressed, Thick-Walled Cylinder of Strain-Hardening Materials," J. of Pressure Vessel Technology, Vol. 105, 1983, pp. 117-123.

20. Parker, A. P. and Andrasic, C. P., "Stress Intensity Prediction For a Multiply-Cracked, Pressurized Gun Tube With Residual and Thermal Stresses," U.S. Army Symposium on Solid Mechanics, AMMRC MS 80-5, 1980, pp. 35-39.

21. Pu, S. L., "Stress Intensity Factors for Radial Cracks at Outer Surface of a Partially Autofrettaged Cylinder Subjected to Internal Pressure," ARRADCOM Technical Report No. ARLCB-TR-82003, Benet Weapons Laboratory, Watervliet, NY, May 1982.

22. Underwood, J. H. and Throop, J. F., "Surface Crack K-Estimates and Fatigue Life Prediction," ASTM STP 687, 1979, pp. 195-210.

23. Pu, S. L. "A Functional Stress Intensity Approach to Multiply-Cracked, Partially Autofrettaged Cylinders," Transactions of the 28th Conference of Army Mathematicians, ARO Report 83-1, 1983, pp. 263-283.

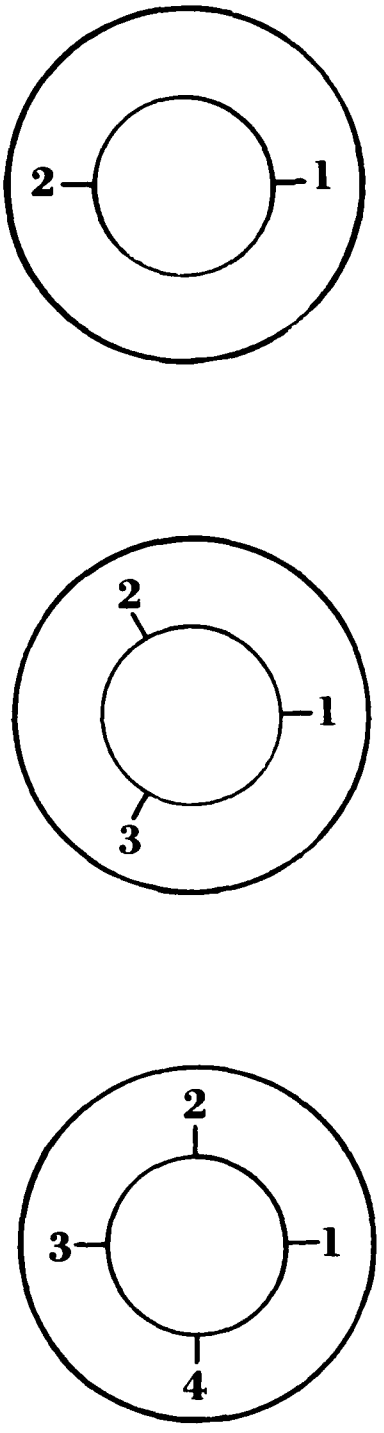

Figure 1. Schematic graphs of a thick-wall cylinder containing two, three, or four radial cracks.

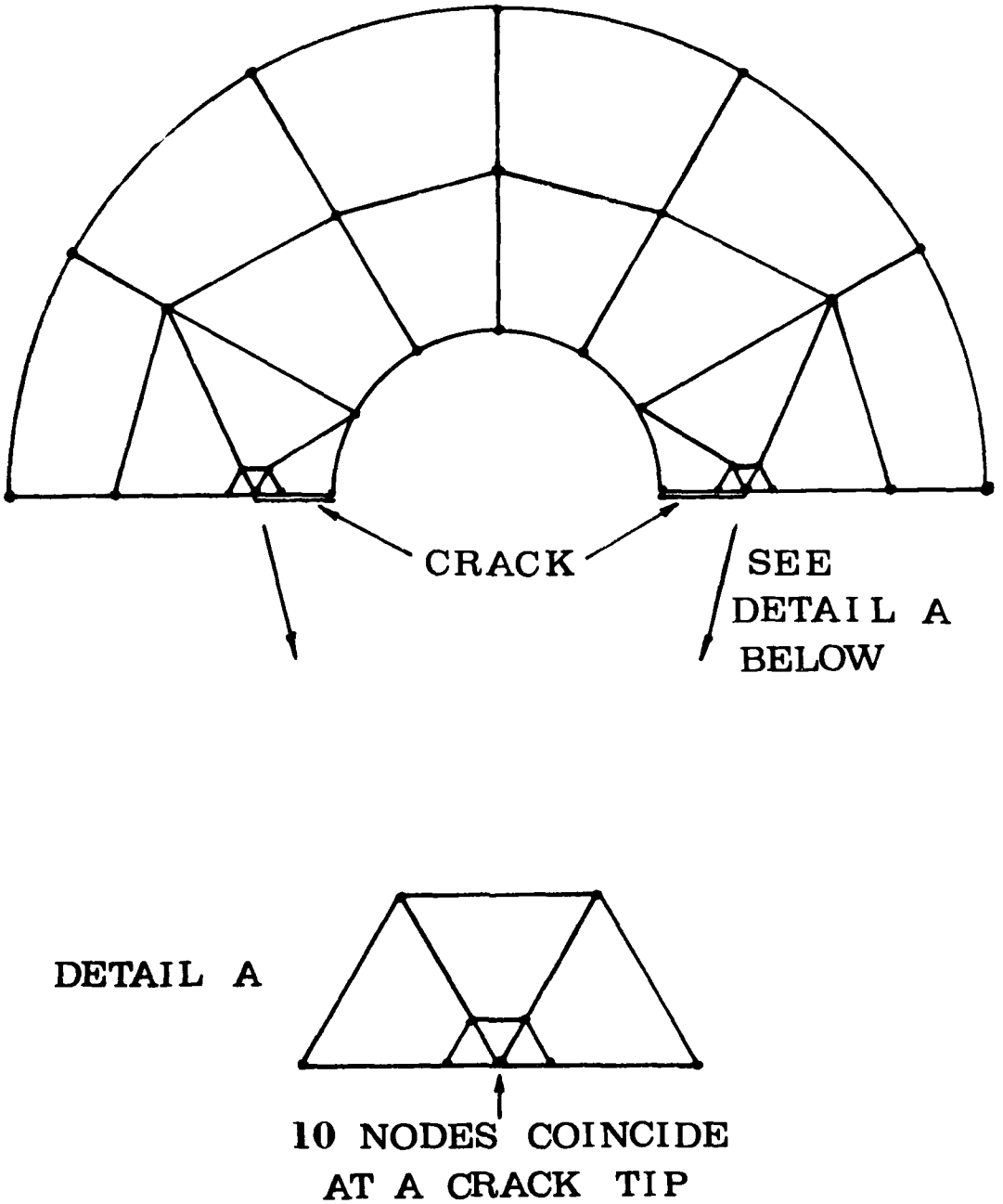

Figure 2. Finite element idealization for two diametrically opposite cracks of unequal depths.

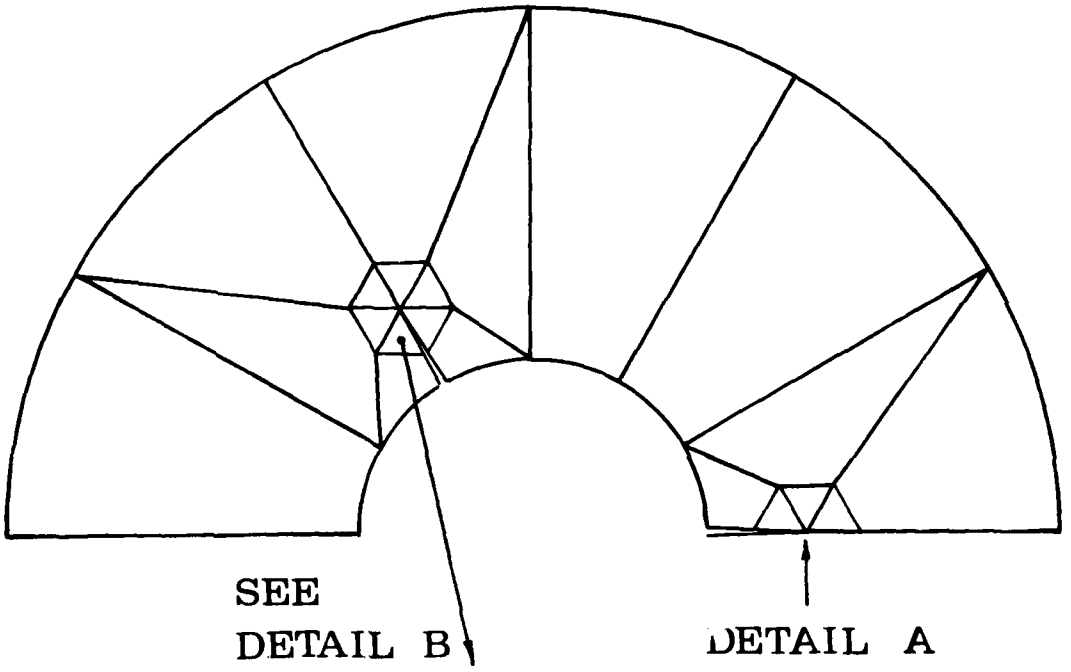

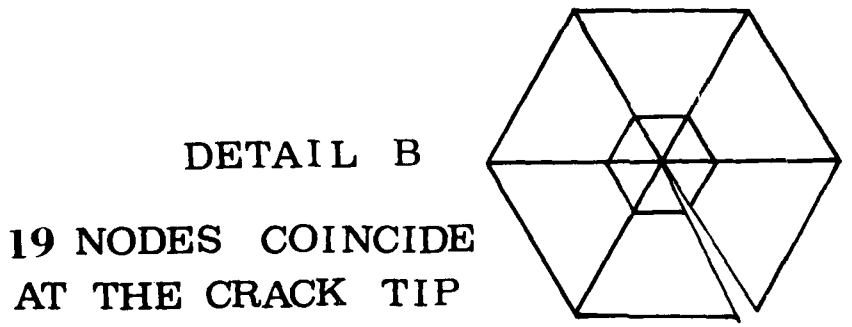

Figure 3. Finite element idealization for a symmetric, three-crack problem.

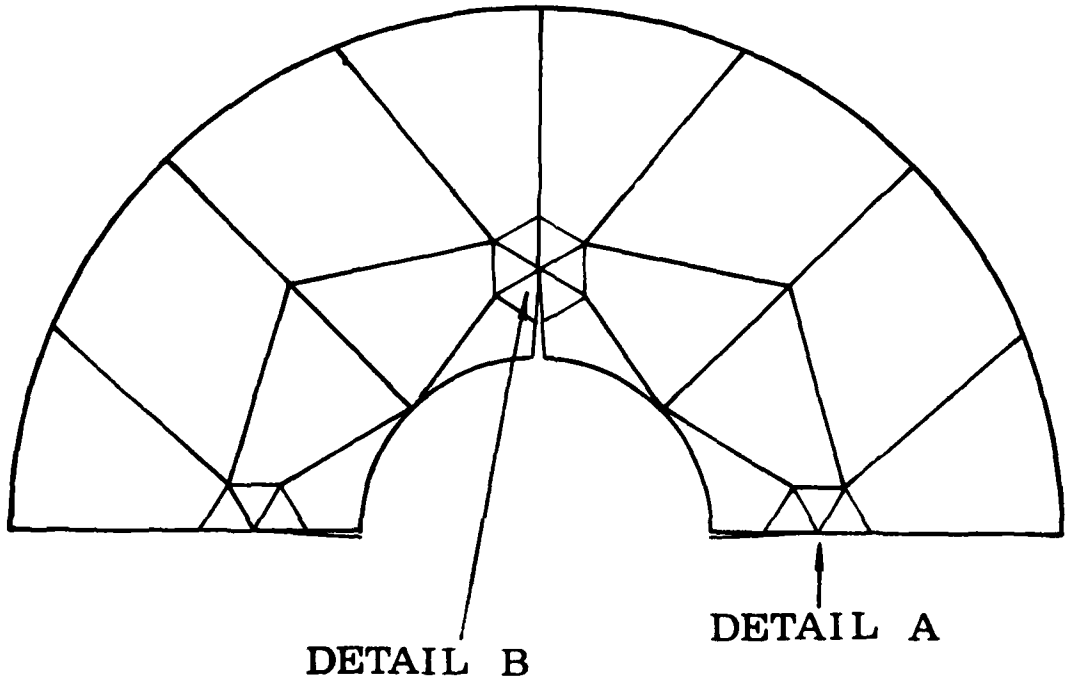

Figure 4. Finite element idealization for a symmetric, four-crack problem.

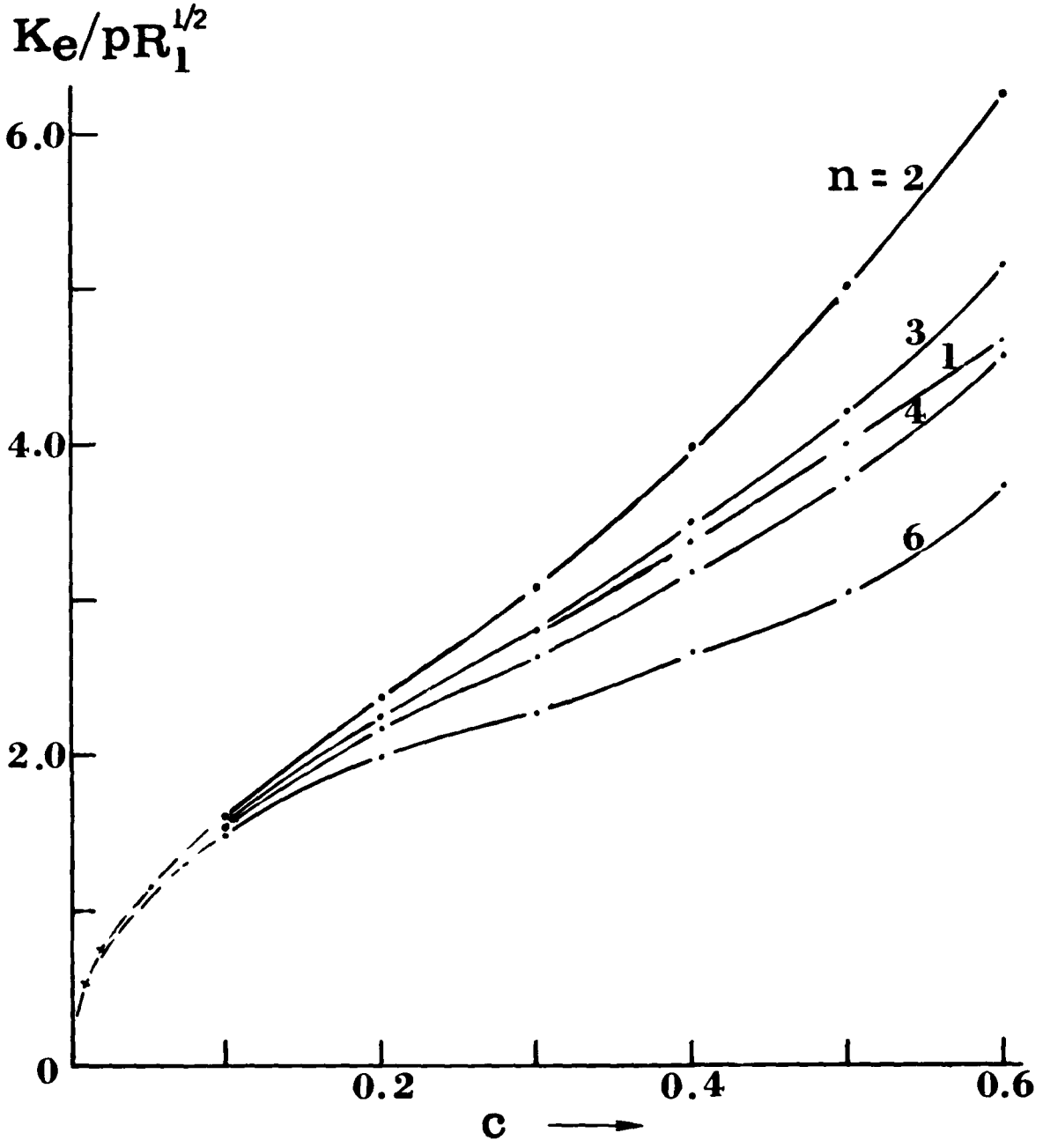

Figure 5. Stress intensity factors as function of crack depth for various numbers of radial cracks of equal depth.

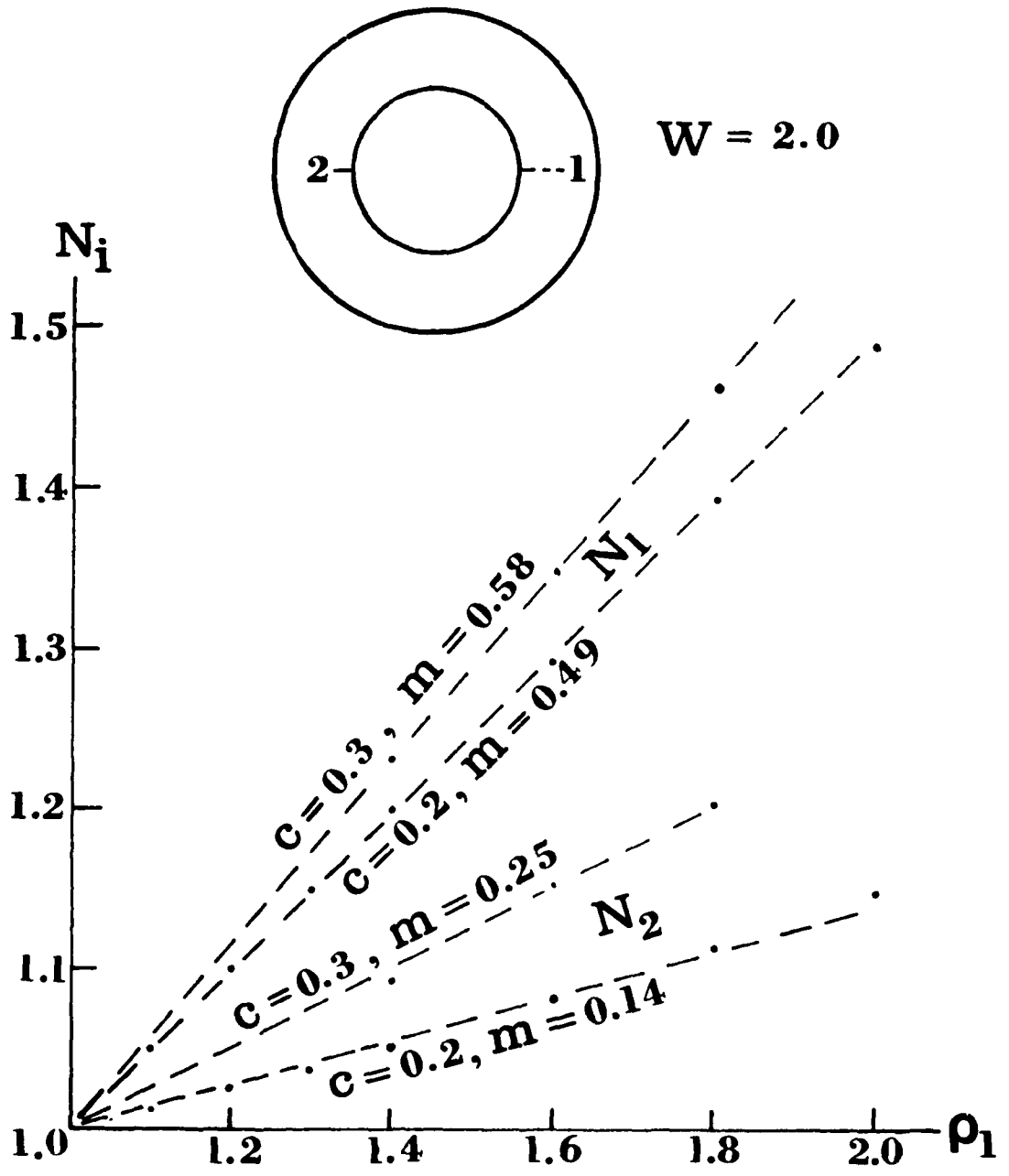

Figure 6. Stress intensity ratio, $N_i = K_i/K_e$, versus crack depth ratio, $\rho_i = c_i/c$, for symmetric two-crack cases.

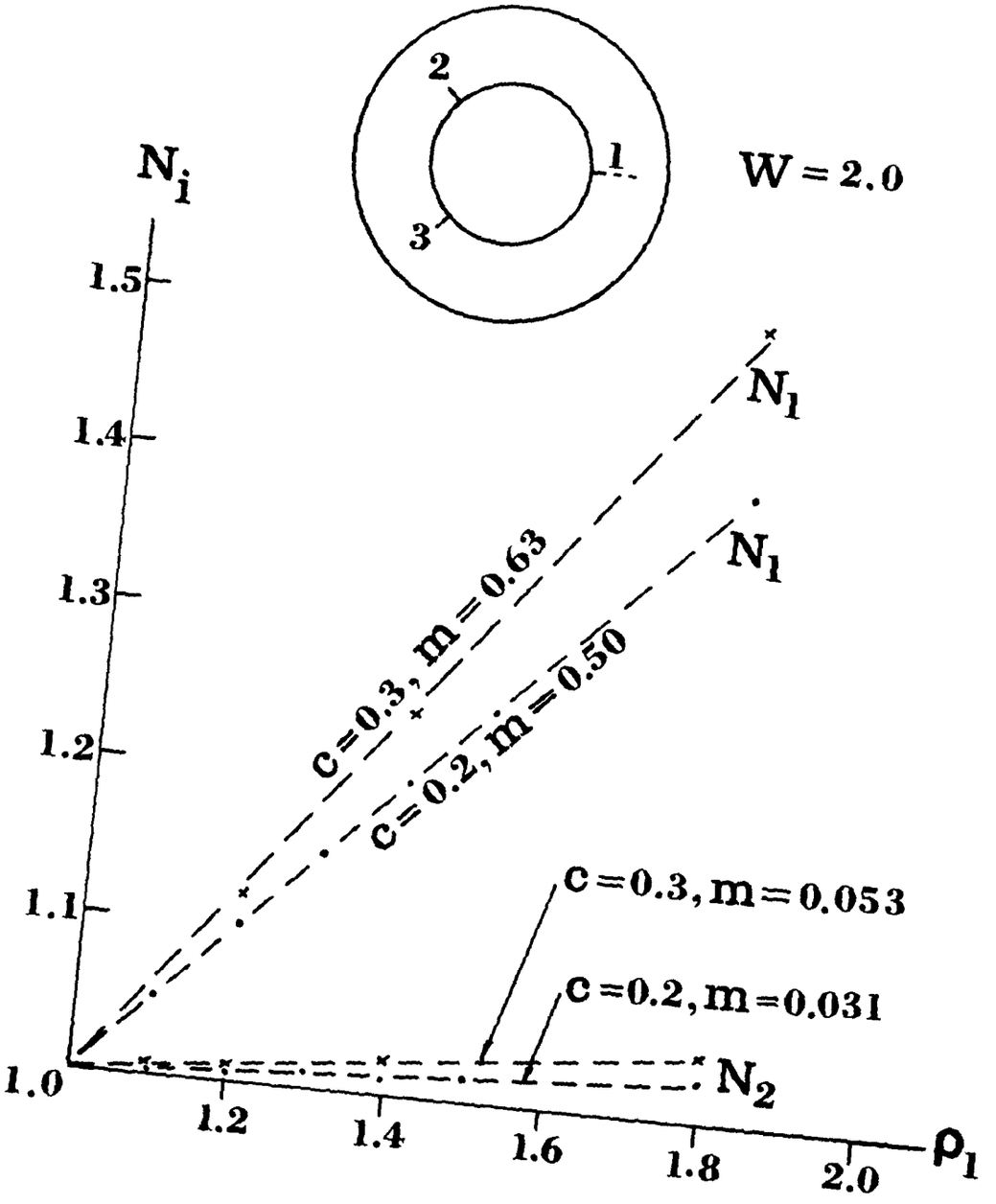

Figure 7. Stress intensity ratio, $N_1 = K_1/K_e$, versus crack depth ratio, $\rho_1 = c_1/c$, for symmetric three-crack cases.

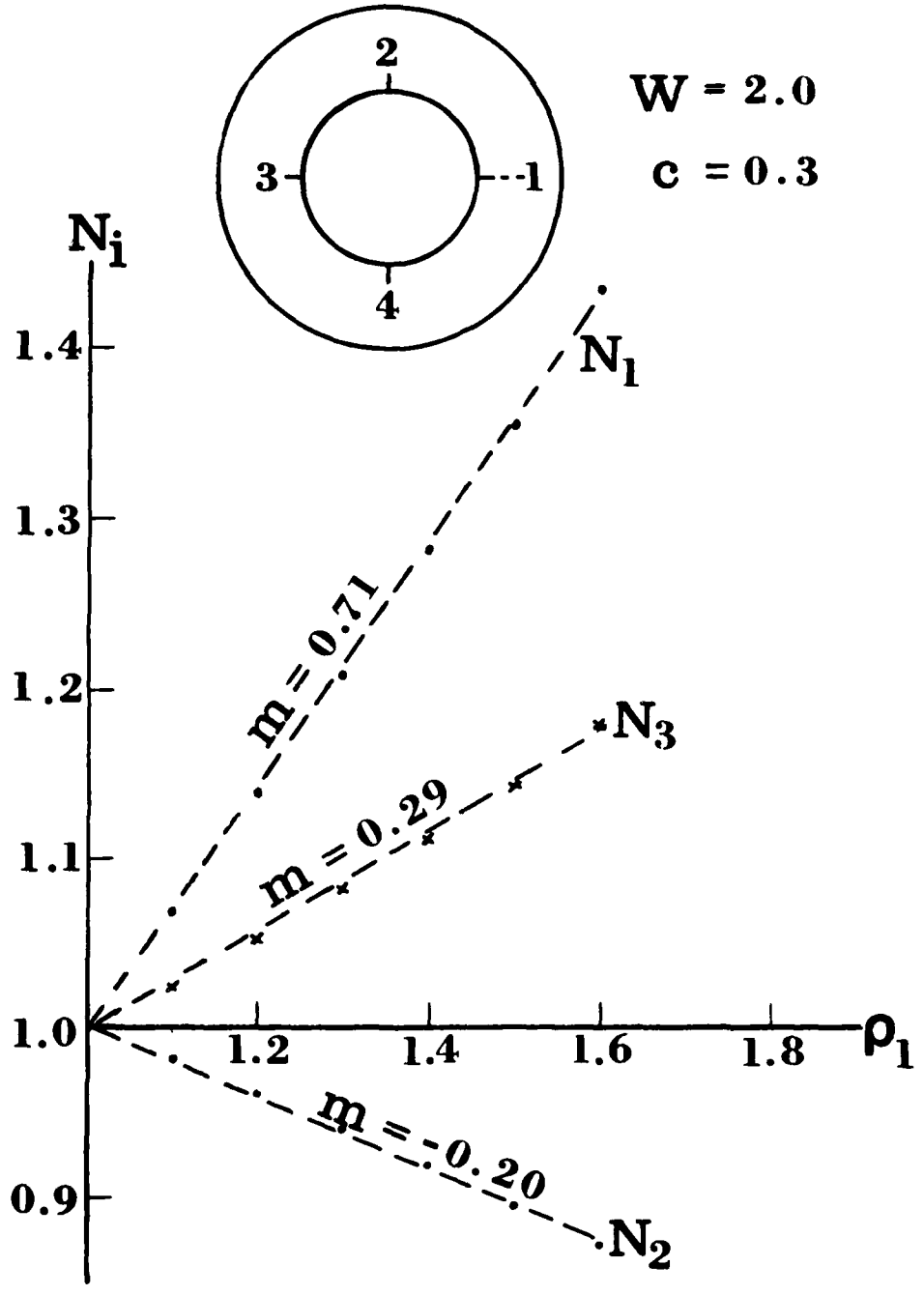

Figure 8. Stress intensity ratio, $N_i = K_i/K_e$, versus crack depth ratio, $\rho_i = c_i/c$, for symmetric four-crack cases.

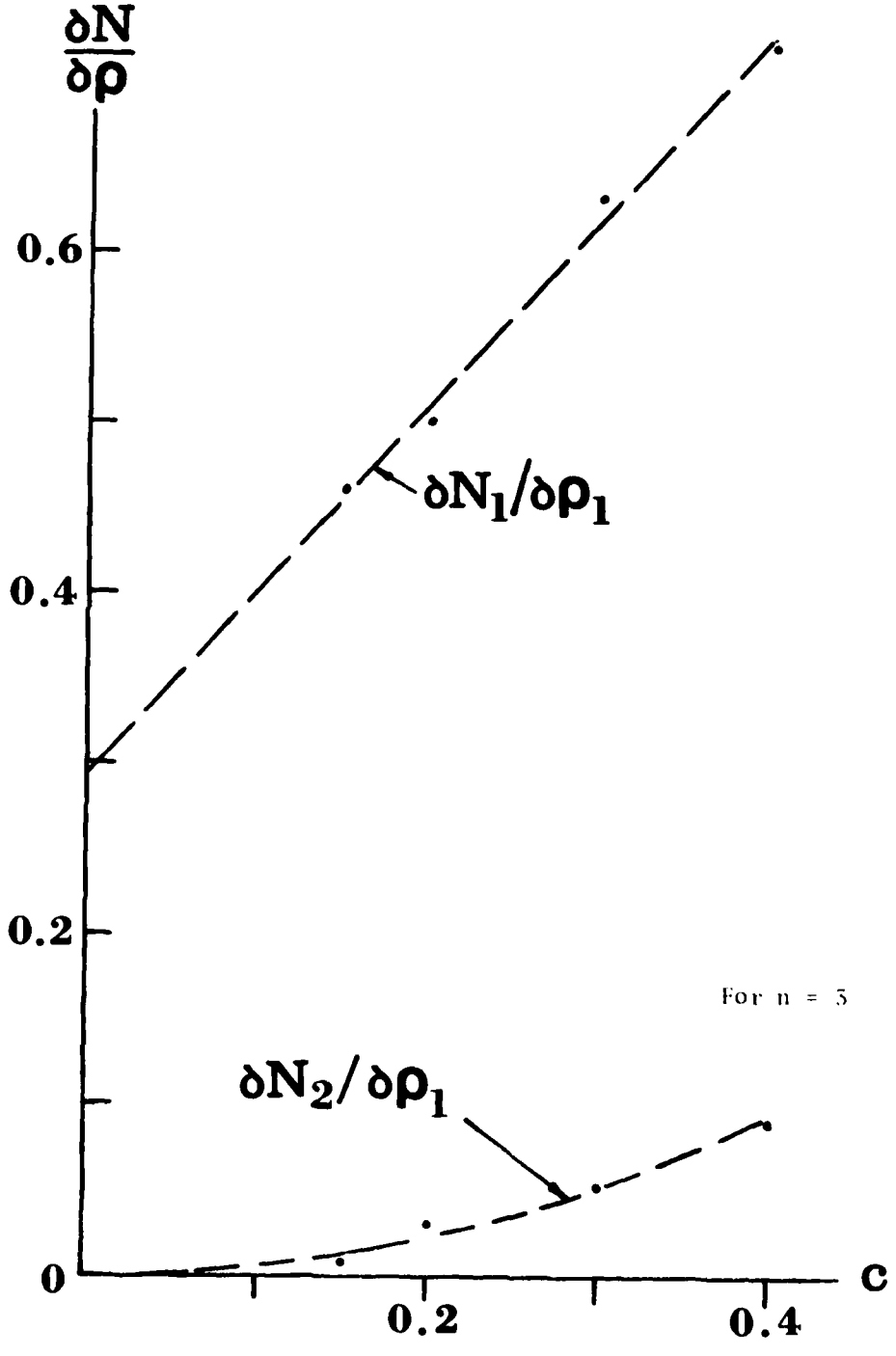

Figure 9. An approximate graph of $\partial N_1/\partial \rho_1$ and $\partial N_2/\partial \rho_1$ as a function of crack depth c for symmetric three radial cracks in a cylinder of wall ratio w = 2.

TECHNICAL REPORT INTERNAL DISTRIBUTION LIST

	NO. OF COPIES
CHIEF, DEVELOPMENT ENGINEERING BRANCH	
ATTN: DRSMC-LCB-D	1
-DP	1
-DR	1
-DS (SYSTEMS)	1
-DS (ICAS GROUP)	1
-DC	1
CHIEF, ENGINEERING SUPPORT BRANCH	
ATTN: DRSMC-LCB-S	1
-SE	1
CHIEF, RESEARCH BRANCH	
ATTN: DRSMC-LCB-R	2
-R (ELLEN FOGARTY)	1
-RA	1
-RM	2
-RP	1
-RT	1
TECHNICAL LIBRARY	5
ATTN: DRSMC-LCB-TL	
TECHNICAL PUBLICATIONS & EDITING UNIT	2
ATTN: DRSMC-LCB-TL	
DIRECTOR, OPERATIONS DIRECTORATE	1
DIRECTOR, PROCUREMENT DIRECTORATE	1
DIRECTOR, PRODUCT ASSURANCE DIRECTORATE	1

NOTE: PLEASE NOTIFY DIRECTOR, BENET WEAPONS LABORATORY, ATTN: DRSMC-LCB-TL, OF ANY ADDRESS CHANGES.

TECHNICAL REPORT EXTERNAL DISTRIBUTION LIST

	NO. OF COPIES
ASST SEC OF THE ARMY RESEARCH & DEVELOPMENT ATTN: DEP FOR SCI & TECH THE PENTAGON WASHINGTON, D.C. 20315	1
COMMANDER DEFENSE TECHNICAL INFO CENTER ATTN: DTIC-DDA CAMERON STATION ALEXANDRIA, VA 22314	12
COMMANDER US ARMY MAT DEV & READ COMD ATTN: DRCDE-SG 5001 EISENHOWER AVE ALEXANDRIA, VA 22333	1
COMMANDER ARMAMENT RES & DEV CTR US ARMY AMCCOM ATTN: DRSMC-LC(D)	1
DRSMC-LCE(D)	1
DRSMC-LCM(D) (BLDG 321)	1
DRSMC-LCS(D)	1
DRSMC-LCU(D)	1
DRSMC-LCW(D)	1
DRSMC-SCM-O (PLASTICS TECH EVAL CTR, BLDG. 351N)	1
DRSMC-TSS(D) (STINFO) DOVER, NJ 07801	2
DIRECTOR BALLISTICS RESEARCH LABORATORY ARMAMENT RESEARCH & DEV CTR US ARMY AMCCOM ATTN: DRSMC-TSB-S (STINFO) ABERDEEN PROVING GROUND, MD 21005	1
MATERIEL SYSTEMS ANALYSIS ACTV ATTN: DRSXY-MP ABERDEEN PROVING GROUND, MD 21005	1
COMMANDER US ARMY AMCCOM ATTN: DRSMC-LEP-L(R) ROCK ISLAND, IL 61299	1
COMMANDER ROCK ISLAND ARSENAL ATTN: SMCRI-ENM (MAT SCI DIV) ROCK ISLAND, IL 61299	1
DIRECTOR US ARMY INDUSTRIAL BASE ENG ACTV ATTN: DRXIB-M ROCK ISLAND, IL 61299	1
COMMANDER US ARMY TANK-AUTMV R&D COMD ATTN: TECH LIB - DRSTA-TSL WARREN, MI 48090	1
COMMANDER US ARMY TANK-AUTMV COMD ATTN: DRSTA-RC WARREN, MI 48090	1
COMMANDER US MILITARY ACADEMY ATTN: CHMN, MECH ENGR DEPT WEST POINT, NY 10996	1
US ARMY MISSILE COMD REDSTONE SCIENTIFIC INFO CTR ATTN: DOCUMENTS SECT, BLDG. 4484 REDSTONE ARSENAL, AL 35898	2
COMMANDER US ARMY FGN SCIENCE & TECH CTR ATTN: DRXST-SD 220 7TH STREET, N.E. CHARLOTTESVILLE, VA 22901	1

NOTE: PLEASE NOTIFY COMMANDER, ARMAMENT RESEARCH AND DEVELOPMENT CENTER, US ARMY AMCCOM, ATTN: BENET WEAPONS LABORATORY, DRSMC-LCB-TL, WATERVLIET, NY 12189, OF ANY ADDRESS CHANGES.

TECHNICAL REPORT EXTERNAL DISTRIBUTION LIST (CONT'D)

	NO. OF COPIES
COMMANDER US ARMY MATERIALS & MECHANICS RESEARCH CENTER ATTN: TECH LIB - DRXMR-PL WATERTOWN, MA 01272	2
COMMANDER US ARMY RESEARCH OFFICE ATTN: CHIEF, IPO P.O. BOX 12211 RESEARCH TRIANGLE PARK, NC 27709	1
COMMANDER US ARMY HARRY DIAMOND LAB ATTN: TECH LIB 2800 POWDER MILL ROAD ADELPHIA, MD 20783	1
COMMANDER NAVAL SURFACE WEAPONS CTR ATTN: TECHNICAL LIBRARY CODE X212 DAHLGREN, VA 22448	1
DIRECTOR US NAVAL RESEARCH LAB ATTN: DIR, MECH DIV CODE 26-27, (DOC LIB) WASHINGTON, D.C. 20375	1 1
COMMANDER AIR FORCE ARMAMENT LABORATORY ATTN: AFATL/DLJ AFATL/DLJG EGLIN AFB, FL 32542	1 1
METALS & CERAMICS INFO CTR BATTELLE COLUMBUS LAB 505 KING AVENUE COLUMBUS, OH 43201	1

NOTE: PLEASE NOTIFY COMMANDER, ARMAMENT RESEARCH AND DEVELOPMENT CENTER, US ARMY AMCCOM, ATTN: BENET WEAPONS LABORATORY, DRSMC-LCB-TL, WATERVLIET, NY 12189, OF ANY ADDRESS CHANGES.


ATE
LME